2013 European Control Conference (ECC)
July 17-19, 2013, Zürich, Switzerland.

Collocation Methods for Multi-Vehicle Trajectory Optimization

Oliver Turnbull*†, Arthur Richards*‡
*Department of Aerospace Engineering, University of Bristol
Queens Building, University Walk, Bristol, BS8 1TR, UK
†Research Assistant, Email: oliver.turnbull@bristol.ac.uk
‡Lecturer, Email: arthur.richards@bristol.ac.uk

***Abstract*—Direct collocation offers an efficient way of transcribing optimal control problems to form nonlinear optimizations. Collocation is particularly attractive for variable time problems as the finishing time can be made a decision variable. However, this causes problems in coupled multi-vehicle problems, for example, where different vehicles may have different finishing times. This paper proposes a way of capturing coupling constraints - in particular, collision avoidance - between vehicles without requiring a common time of arrival. The approach exploits a recently-developed dualization approach for avoidance constraints, extended to act time as well as spatial dimensions.**

I. Introduction

An increasing number of problems are modelled with nonlinear system dynamics such as UAV path planning [1], [2] and Air Traffic Management (ATM) [3], [4] to industrial processes such as polymer production [5]. This is reflected in the large volume of research into optimal trajectory generation [1], [6], [7], obstacle [2], [8] and collision avoidance [3], [4], [9], [10]. This paper presents a novel method of multi-vehicle collision avoidance for systems with nonlinear dynamics and in particular, multi-agent systems with coupled constraints and different planning horizons.

Nonlinear optimization is one method that has been proposed for trajectory generation [2], [8] for systems that require nonlinear dynamics models. However, convergence of nonlinear optimizations can be a challenge and global optimality is not guaranteed. One possible solution to these limitations is nonlinear branch and bound [2] which offers the potential to find the global optimal solution to a problem including the full nonlinear dynamics but extension beyond 2-D remains unresolved.

One popular class of nonlinear optimization is collocation methods which approximate the state of an optimal control problem by a basis of polynomials [11] and are an active area of research for problems where it is necessary to model hard nonlinear dynamics [1], [4], [5], [12].

Collocation has often been proposed [1], [4], [5] as a means to model nonlinear dynamics in systems with algebraic constraints, such as for avoidance. However, when applied to multi-vehicle problems, all of these methods require a common planning horizon (start and finish time) for all vehicles, in order to guarantee collision avoidance.

This paper takes the collocation method proposed in [13] and the obstacle avoidance method of Patel and Goulart based on polar sets [8] to develop a nonlinear collision avoidance model. The basic obstacle avoidance model is extended to multi-vehicle collision avoidance and it is shown that by finding a common separating 4-D hyperplane for adjacent time-steps we can achieve inter-sample avoidance. Finally, the avoidance of 4-D obstacles and multi-vehicle collision avoidance are applied to example problems in the ATM domain.

This paper is organized as follows: Section II defines the problem statement and reviews the collocation method; Section III extends the method of [8] to account for 4-D obstacles; Section IV extends the 4-D obstacle avoidance method to collision avoidance of multiple vehicles; both obstacle and collision avoidance are then demonstrated in Section V in the context of ATM along with some computational complexity results; finally some conclusions are drawn in Section VI.

II. Trajectory Optimization by Direct Collocation

A. Problem Statement

Consider a set of N_a aircraft with dynamics and constraints:

$$\dot{\mathbf{x}}(a,t) = f(\mathbf{x}(a,t), \mathbf{u}(a,t), a) \forall\, t, a \tag{1}$$

$$g(\mathbf{x}(a,t), \mathbf{u}(a,t), a) \leq 0 \;\forall\, t, a \tag{2}$$

$$\mathbf{x}(a,0) = \mathbf{x}_0(a) \forall\, a \tag{3}$$

$$\mathbf{x}(a, t_f(a)) = \mathbf{x}_f(a) \forall\, a \tag{4}$$

where $a \in \{1, \ldots, N_a\}$ is the aircraft index and t is time. Observe that all vehicles have the same starting time $t = 0$ but potentially different finishing times $t_f(a)$. It should be noted, however, that the proposed method can also accommodate multiple start times.

In this paper our primary interest is developing a 4-D collocation framework so we define a simple, minimal-time cost function:

$$J = \min \sum_{a \in 1..N_a} t_f(a). \tag{5}$$

B. Collocation Method

Collocation methods use the Lagrange interpolating polynomial to the model dynamics. Collocation methods convert optimal control problems into finite dimensional optimizations, representing the trajectory in polynomial form. However, care must be taken when selecting the collocation points at which the polynomial is evaluated in order to avoid undesirable behaviour between points due to Runge's phenomenon [14].

This paper focuses on extending the applicability of collocation methods to multi-agent problems with coupled constraints between vehicles. An example of a coupled constraint is avoidance: the permissible state/space for one vehicle is dependent on the position of all other vehicles. With a multi-agent system with multiple planning horizons, there is no guarantee that the collocation points for different vehicles will be co-incident in time which prevents a meaningful comparison of position.

To develop such a framework we adopt the collocation method of [13] which is briefly reviewed here. Define a set of normalized time points $\tau_i : i \in \{1, \ldots, N_c\}$ "collocation points" over an interval $\tau \in [-1, 1]$. The "real" time for each vehicle at each collocation point is given by $t_i(a) = \frac{\tau_i+1}{2} t_f(a)$. These individual time scales are what makes it difficult to model constraints coupling two or more vehicles, motivating the development in this paper.

The trajectories $\mathbf{x}(a, t)$ are parameterized by the state values at the collocation points $\mathbf{x}_i(a) = \mathbf{x}(a, t_i(a))$. Then, assuming that the state trajectories follow Lagrange polynomials fitted to the collocation points, we can write

$$\left.\frac{\partial \mathbf{x}(a,t)}{\partial \tau}\right|_{\tau_i} = \sum_j d_{i,j} \mathbf{x}_j(a). \tag{6}$$

where the terms $d_{i,j}$ are from an interpolating matrix that comes from the Vandermonde matrix of order N_c [13]. Hence the differential constraints applied at the collocation points in the optimization can be written as:

$$\sum_j d_{i,j} \mathbf{x}(\tau_j) = \frac{2}{t_f} f(\mathbf{x}_i(a), \mathbf{u}_i(a), a) \ \forall\, i, a \tag{7}$$

Hence the state, $\mathbf{x}_i(a)$, and control values, $\mathbf{u}_i(a)$, at the collocation points are decision variables in the problem.

For efficient solutions, the collocation points are generally not evenly distributed over the interval $[-1, 1]$. Considerable research has been performed on the best distribution of collocation points [13], [15] and this is beyond the scope of this paper. For the inequality constraints, however, a uniform distribution is desired. Therefore, we also define a set of N_e "evaluation points" $t_k(a) = \frac{k-1}{N_e-1} t_f(a)$. Again, interpolating using the Lagrange polynomial, we can relate the states and controls at the evaluation points to those at the collocation points, by:

$$\mathbf{x}(a, t_k(a)) = \sum_j e_{k,j} \mathbf{x}_j(a) \tag{8}$$

$$\mathbf{u}(a, t_k(a)) = \sum_j e_{k,j} \mathbf{u}_j(a). \tag{9}$$

Then the algebraic constraints are applied at these evaluation points:

$$g\left(\sum_j e_{k,j} \mathbf{x}_j(a), \sum_j e_{k,j} \mathbf{u}_j(a), a\right) \leq 0 \ \forall\, k, a \tag{10}$$

Finally the boundary conditions can be rewritten as

$$\sum_j e_{1,j} \mathbf{x}_j(a) = \mathbf{x}_0(a) \forall\, a \tag{11}$$

$$\sum_j e_{N_e,j} \mathbf{x}_j(a) = \mathbf{x}_f(a) \forall\, a \tag{12}$$

The overall optimization becomes

$$J = \min_{\{\mathbf{x}_i(a), \mathbf{u}_i(a), t_f(a)\}_{a,i}} \sum_{a \in 1..N_a} t_f(a) \tag{13}$$

subject to (7), (10), (11) and (12).

The optimization can now be solved using a third party solver such as IPOPT [16]. IPOPT uses an interior point algorithm to solve the nonlinear optimization and as such provides no guarantee of global optimality. Furthermore, the rate of convergence and quality of the solution are highly dependent on the starting point, or initial solution, in the search space. In an attempt to provide a feasible initial solution we initialize the search with a trajectory generated using potential fields [17], [18]. This method is able to rapidly provide an initial solution with limited computational expense, although there are well known limitations [19] and the solution may not be dynamically feasible. Future work could investigate alternative initialization methods to overcome some of the limitations of potential fields, such as susceptibility to local minima, which would improve robustness.

III. Avoidance of 4-D Obstacles

Let $C \subseteq \mathbb{R}^n$ define a convex exclusion region including the origin, i.e. $0 \in C$. Patel and Goulart [8] showed that the avoidance constraint $x \notin C$ is equivalent to $x^T y \geq 1, y \in C^0$ where C^0 is the polar set of C:

$$C^0 \triangleq \{v | \langle v, x \rangle \leq 1, \ \forall\, x \in C\} \tag{14}$$

This provides a differentiable representation of avoidance constraints, compatible with gradient-based nonlinear optimizers, for any convex exclusion region C such as a polyhedron. Fig. 1 shows an example of the polar set of a square obstacle.

We will first exploit this idea to enforce a *4-D obstacle*, an exclusion region which has finite definition in time as well as space. This could represent, for example, a temporary closure of a sector of airspace. Moving obstacles or fixed paths of other vehicles can also be captured in this way. Define $(\mathbf{r}_{obs}, t_{obs})$ as a point within the exclusion in both space and time and define $C \in \Re^4$ such that the exclusion can be written as

$$\begin{pmatrix} \mathbf{r}(a,t) - \mathbf{r}_{obs}(\tau) \\ t - t_{obs} \end{pmatrix} \notin C \ \ \forall t \tag{15}$$

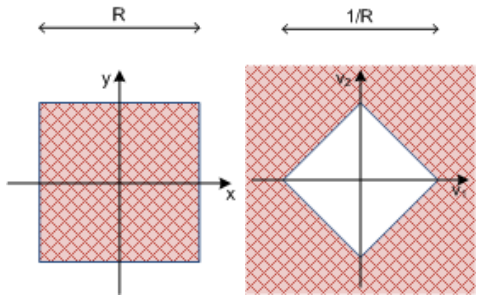

(a) (b)

Fig. 1. A square obstacle in Cartesian and polar spaces

To simplify notation, denote the position of aircraft a at its evaluation point $t_k(a)$ by $r_k(a)$, which can be determined from the collocation decision variables using (8). Thus $r_k(a)$ are effectively decision variables, fixed to the collocation points $x_j(a)$ by equality constraints, although in practice r is eliminated by substitution. Then, adopting the dualization approach, the avoidance constraints can be enforced at each evaluation point in the form

$$\mathbf{y}_k(a)^T \begin{pmatrix} \mathbf{r}_k(a) - \mathbf{r}_{obs} \\ t_k(a) - t_{obs} \end{pmatrix} \geq 1 \ \forall \ k \tag{16}$$

and

$$\mathbf{y}_k(a) \in C^0 \tag{17}$$

where the dual variables $\mathbf{y}_k(a)$ are additional decision variables in the problem.

As the constraints are only enforced at the evaluation points, there is a risk of the trajectory cutting into the obstacle between two adjacent time samples. To mitigate this problem, we add extra constraints requiring avoidance with the same dual variable $\mathbf{y}_k(a)$ at the preceding time step $k-1$:

$$\mathbf{y}_k(a)^T \begin{pmatrix} \mathbf{r}_{k-1}(a) - \mathbf{r}_{obs} \\ t_{k-1}(a) - t_{obs} \end{pmatrix} \geq 1 \ \forall \ k \tag{18}$$

Interpreting $\mathbf{y}_k(a)^T\mathbf{x} \geq 1$ as a hyperplane separating the trajectory from the obstacle, (18) ensures that there is a common hyperplane between the trajectory and the obstacle at points $k-1$ and k. Hence, no point on a line joining $\mathbf{r}_{k-1}(a)$ and $\mathbf{r}_k(a)$ can be inside the obstacle. This doesn't completely remove the possibility of incursion but it does make it highly improbable. This approach is analogous to the approach of Maia and Galvao [20] to prevent inter-sample incursion using Mixed-Integer Linear Programming (MILP) for avoidance optimization. Indeed, the dualization approach is related to the MILP method, which selects separating hyperplanes using binary variables. Further discussion of this topic is beyond the scope of this paper.

IV. Multi-Vehicle Collision Avoidance

This section extends the 4-D avoidance method to enforce avoidance between two vehicles. Consider the avoidance constraint first in spatial form

$$\mathbf{r}(a,t) - \mathbf{r}(b,t) \notin \mathcal{A} \ \forall t \tag{19}$$

for a pair of aircraft a and b where $\mathcal{A}$ is the definition of the exclusion zone around each aircraft. We cannot express this directly in the collocation optimization because the states are not evaluated at a common set of times for all vehicles, meaning $t_k(a) \neq t_k(b)$ in general. Therefore, consider instead the augmented 4-D constraint

$$\begin{pmatrix} \mathbf{r}_k(a) - \mathbf{r}_j(b) \\ t_k(a) - t_j(b) \end{pmatrix} \notin \mathcal{A} \times \{0\} \quad \forall k, j, a > b \tag{20}$$

which fails (i.e. indicates conflict) if any two points on the trajectories of a and b are in the exclusion zone at the same time. Defining the 4-D conflict set as $\mathcal{C} = \mathcal{A} \times \{0\}$, it is clear that it is convex so the dualization method can be applied. The dual set is given by

$$\mathcal{C}^0 = \mathcal{A}^0 \times \Re \tag{21}$$

where the infinite extent in the time dimension is, loosely, the "reciprocal" of the zero width in the time dimension of the original conflict set. Hence the avoidance constraint can be written as

$$\mathbf{y}_{kj}(a,b)^T \begin{pmatrix} \mathbf{r}_k(a) - \mathbf{r}_j(b) \\ t_k(a) - t_j(b) \end{pmatrix} \geq 1 \quad \forall k, j, a > b \tag{22}$$

with

$$[\mathbf{I}_3 \mathbf{0}_{3\times 1}]\, \mathbf{y}_{kj}(a,b)^T \in \mathcal{A}^0 \tag{23}$$

The above will enforce spatial avoidance if two evaluation points exactly co-incide. However, this is unlikely, so the inter-sample behaviour will dominate. The 4-D obstacle example identified that the key to inter-sample avoidance is to ensure a common hyperplane between time steps. To see how this extends to the multi-vehicle case, consider the following proposition.

Theorem Assume there exists a dual variable $\mathbf{y}$ such that

$$\mathbf{y}^T(\mathbf{v}_1 - \mathbf{w}_1) \geq 1 \tag{24a}$$
$$\mathbf{y}^T(\mathbf{v}_2 - \mathbf{w}_1) \geq 1 \tag{24b}$$
$$\mathbf{y}^T(\mathbf{v}_1 - \mathbf{w}_2) \geq 1 \tag{24c}$$
$$\mathbf{y}^T(\mathbf{v}_2 - \mathbf{w}_2) \geq 1. \tag{24d}$$

Then for any pair of points, $\mathbf{v}_3$ on the line from $\mathbf{v}_1$ to $\mathbf{v}_2$ and $\mathbf{w}_3$ on the line from $\mathbf{w}_1$ to $\mathbf{w}_2$, the following holds: $\mathbf{y}^T(\mathbf{v}_3 - \mathbf{w}_3) \geq 1$.

Proof The two intermediate points can be written as

$$\mathbf{v}_3 = \alpha\mathbf{v}_1 + (1-\alpha)\mathbf{v}_2, \ \alpha \in [0,1] \tag{25}$$
$$\mathbf{w}_3 = \beta\mathbf{w}_1 + (1-\beta)\mathbf{w}_2, \ \beta \in [0,1] \tag{26}$$

Using (25), we can write

$$\mathbf{y}^T(\mathbf{v}_3 - \mathbf{w}_3) = \mathbf{y}^T(\alpha(\mathbf{v}_1 - \mathbf{w}_3) + (1-\alpha)(\mathbf{v}_2 - \mathbf{w}_3)) \tag{27}$$
$$= \alpha\mathbf{y}^T(\mathbf{v}_1 - \mathbf{w}_3) + (1-\alpha)\mathbf{y}^T(\mathbf{v}_2 - \mathbf{w}_3) \tag{28}$$

which must be between $\mathbf{y}^T(\mathbf{v}_1 - \mathbf{w}_3)$ and $\mathbf{y}^T(\mathbf{v}_2 - \mathbf{w}_3)$ implying

$$\mathbf{y}^T(\mathbf{v}_3 - \mathbf{w}_3) \geq \min\{\mathbf{y}^T(\mathbf{v}_1 - \mathbf{w}_3), \mathbf{y}^T(\mathbf{v}_2 - \mathbf{w}_3)\} \tag{29}$$

Now subsititute for $\mathbf{w}_3$ using (26) in both terms in the minimum in (29):

$$\mathbf{y}^T(\mathbf{v}_1 - \mathbf{w}_3) = \beta \mathbf{y}^T(\mathbf{v}_1 - \mathbf{w}_1) + (1-\beta)\mathbf{y}^T(\mathbf{v}_1 - \mathbf{w}_2) \tag{30}$$

$$\mathbf{y}^T(\mathbf{v}_2 - \mathbf{w}_3) = \beta \mathbf{y}^T(\mathbf{v}_2 - \mathbf{w}_1) + (1-\beta)\mathbf{y}^T(\mathbf{v}_2 - \mathbf{w}_2) \tag{31}$$

From (24) we know that this is the convex combination of terms all greater than or equal to one. Hence $\mathbf{y}^T(\mathbf{v}_1 - \mathbf{w}_3) \geq 1$ and $\mathbf{y}^T(\mathbf{v}_2 - \mathbf{w}_3) \geq 1$ and looking back at (29), these imply $\mathbf{y}^T(\mathbf{v}_3 - \mathbf{w}_3) \geq 1$. ■

The Theorem shows that if the same dual constraint is applied to time step pairs $(t_k(a), t_j(b))$, $(t_{k-1}(a), t_j(b))$, $(t_k(a), t_{j-1}(b))$ and $(t_{k-1}(a), t_{j-1}(b))$, then no points in the intervals $[t_{k-1}(a), t_k(a)]$ and $[t_{j-1}(b), t_j(b)]$ can be in conflict, assuming linear motion between samples. Hence the multi-vehicle collision avoidance can be enforced by (22) and (23) in combination with the following three additional constraints $\forall k > 1, j > 1, a > b$:

$$\mathbf{y}_{kj}(a,b)^T \begin{pmatrix} \mathbf{r}_{k-1}(a) - \mathbf{r}_j(b) \\ t_{k-1}(a) - t_j(b) \end{pmatrix} \geq 1 \tag{32}$$

$$\mathbf{y}_{kj}(a,b)^T \begin{pmatrix} \mathbf{r}_k(a) - \mathbf{r}_{j-1}(b) \\ t_k(a) - t_{j-1}(b) \end{pmatrix} \geq 1 \tag{33}$$

$$\mathbf{y}_{kj}(a,b)^T \begin{pmatrix} \mathbf{r}_{k-1}(a) - \mathbf{r}_{j-1}(b) \\ t_{k-1}(a) - t_{j-1}(b) \end{pmatrix} \geq 1 \tag{34}$$

Taken altogether, applied across all pairs of evaluation points, these constraints imply that at no point on the trajectory, interpolated between the evaluation points, are the 4-D avoidance constraints violated. Figure 2 illustrates these constraints for the simplified 1-D + time case.

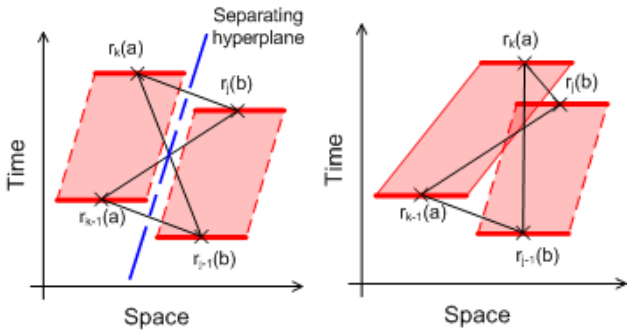

(a) Collision free (b) Conflicting

Fig. 2. Illustration of inter-sample avoidance criteria

The linear motion assumption requires evaluation points to be relatively close together. Note that evaluation points can be added without increasing the number of collocation points and hence decision variables; at the expense of more constraints.

V. Air Traffic Control Examples

Section V-A applies collocation to a 6DOF point mass aircraft model and demonstrates avoidance of a 4-D obstacle such as a temporarily closed region of airspace. Section V-B demonstrates multi-vehicle collision avoidance using a simplified 2-D plus time aircraft model. The simplified model was used to enable a better initialization and to improve the clarity of the results.

A. Avoidance of 4-D Obstacles

Applying the above formulation to a single aircraft and two obstacles we can see the possible effects of the obstacles temporal nature on the aircraft trajectories. Figure 3 shows an example of 4-D obstacle avoidance trajectories where the trajectory is defined by seven collocation points and with constraints enforced at twenty evaluation points. The trajectory is shown projected onto the X-Y plane in Figure 3(a); the small shaded obstacle exists for the duration of the trajectory while the large obstacle must only be avoided for the first 360 seconds as indicated in Figure 3(b) which shows the evolution over time of the aircraft's position and the location of the large obstacle in the x-direction, such that the aircraft is prohibited from entering the shaded region. The trajectory is an example of a situation where the required deviation around an obstacle is so large that it is "cheaper" to wait until such a time that the trajectory can pass straight through the obstacle; the curve in the path prior to entering the large obstacle is due to the weightings of the cost function favouring a minimum time solution, by constantly accelerating whilst waiting for the obstacle to disappear the time required after that point can then be minimized.

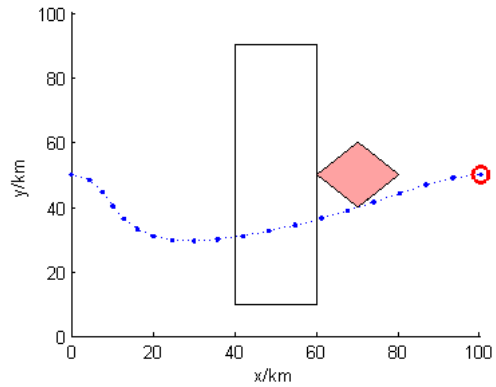

(a) Aircraft trajectory

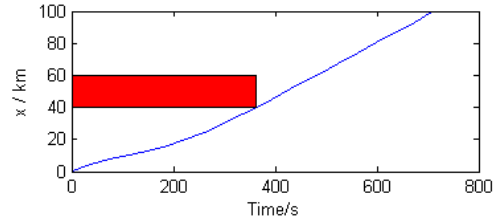

(b) Position of aircraft and temporal obstacle in x-dimension

Fig. 3. Example of a trajectory avoiding a 4-D obstacle

B. Multi-Vehicle Avoidance

Figure 4 shows three examples using the multi-vehicle avoidance optimization from Section IV, initialized with a simple interpolation between initial and final positions.

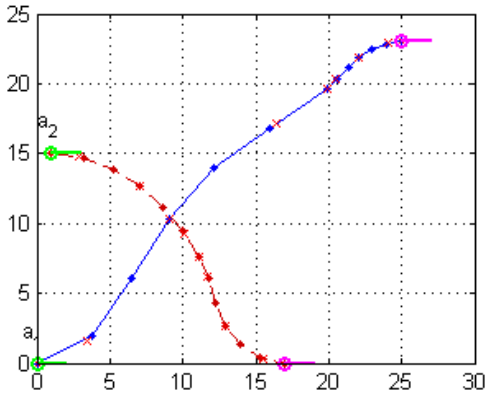

(a) Vehicle Trajectories - 2 vehicle case

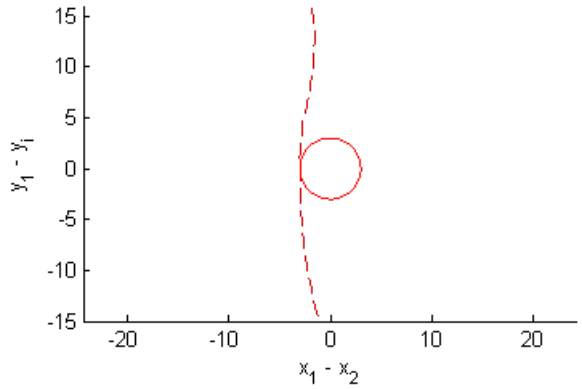

(b) Motion of Aircraft 2 relative to Aircraft 1

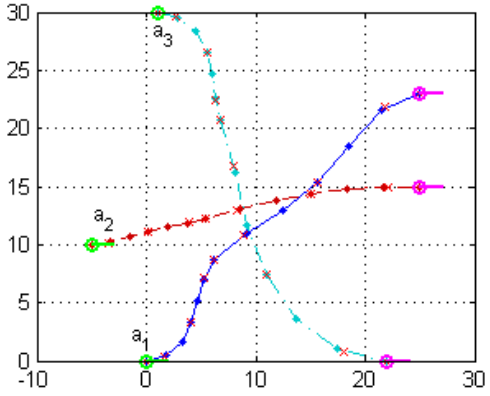

(c) Vehicle Trajectories - 3 vehicle case

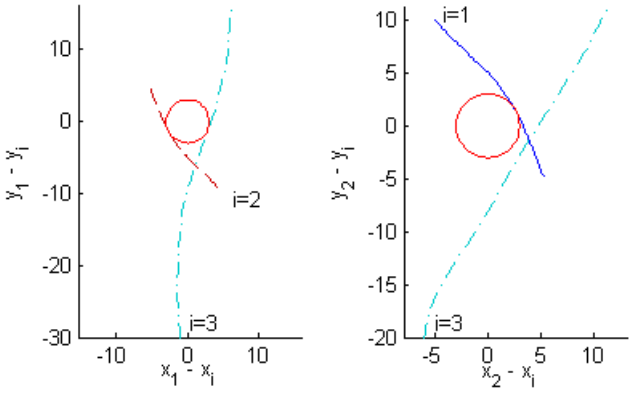

(d) Relative motion of aircraft

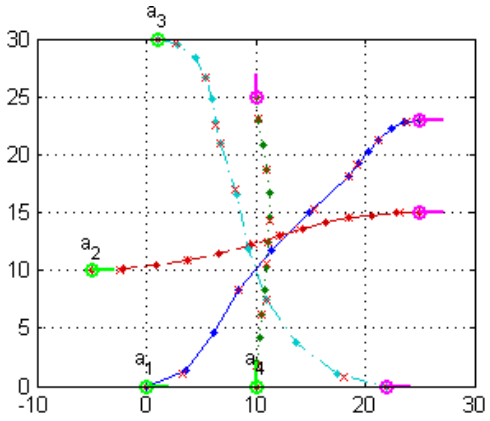

(e) Vehicle Trajectories - 4 vehicle case

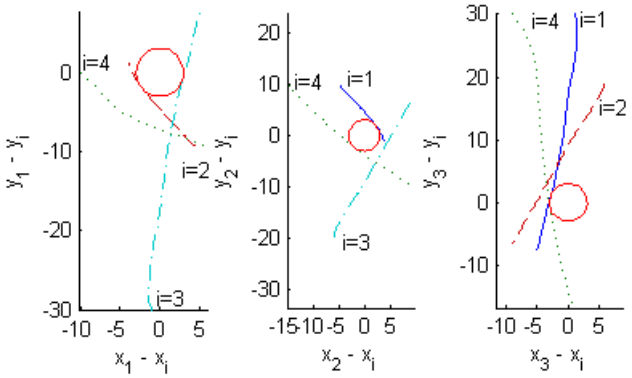

(f) Relative motion of aircraft

Fig. 4. Example of Multi-Vehicle Avoidance

The optimized trajectories all consist of two elements, each defined by five collocation points and with constraints enforced at seven evaluation points. For each example, there are plots showing the trajectories of the aircraft and also a plot showing the relative motion between all aircraft, found by interpolating the optimized trajectories over a common fine time-scale. The relative position plots clearly indicate the avoidance region the other aircraft must avoid.

Figures 4(a) and 4(b) show a 2 aircraft case where the trajectories cross paths and the aircraft have different distances to their destinations. The longer flight takes 19 seconds while the shorter only takes 11 and both can be seen to deviate to avoid collision. All the trajectories are discretized using 7 collocation points and 7 evaluation points. This is an extremely coarse discretization, as can be seen in the trajectory plot, Figure 4(a), but it serves to show the effect

of the constraints on inter-sample behaviour.

Figures 4(c) and 4(d) show a 3 aircraft example where multiple crossing points occur. The finishing times of the aircraft are 19, 15 and 20 seconds for a_1 to a_3 respectively. The final example in Figures 4(e) and 4(f) introduces an additional vehicle into the previous case which requires a_1 to initially be delayed resulting in a longer trajectory (29 seconds) but there is no significant affect on the other aircraft.

The relative motion plots show that in all cases there is no cutting into the avoidance region. Furthermore, from the proximity of the trajectories to the conflict region it is clear that the "obstacle" has been accurately captured.

To provide an indication of the computational complexity of the proposed algorithms solution times to the multi-vehicle collision avoidance examples presented in the paper are shown in Table I. All examples were solved using AMPL and IPOPT on a 3.4GHz, quad core desktop PC with 3GB of RAM.

TABLE I
EXAMPLE OPTIMIZATION SOLVE TIMES

	Solve Time
1: 2 vehicles (Fig. 4(a))	1.015
2: 3 vehicles (Fig. 4(c))	5.564
3: 4 vehicles (Fig. 4(e))	20.157

Table I shows that the computational complexity of the collision avoidance algorithm is relatively low allowing rapid path planning.

VI. CONCLUSIONS

This paper has demonstrated a collocation method for collision avoidance between vehicles planning over independent horizons by defining a common hyperplane, in the vehicles dual space, to separate adjacent pairs of time-steps. This development was facilitated by the generalization of polar obstacles to 4-D which allows us to explicitly include time in our avoidance criteria.

The proposed method allows collocation methods to be applied more intuitively to a broad range of problems where the agents have different planning horizons, i.e. they have different start and finish times.

Due to the nature of nonlinear optimization, the quality and computational effort required for each solution is heavily dependent on the initial guess supplied to the optimizer. Future work could include investigation of methods for more intelligent initialization with the goal of improving speed and robustness.

ACKNOWLEDGEMENT

This work was conducted as part of a larger research effort entitled SUPErvision of Route Optimizers (SUPEROPT). The SUPEROPT project is funded by the SESAR program within Work Package E.

REFERENCES

[1] K. Misovec, T. Inanc, J. Wohletz, and R. Murray, "Low-observable nonlinear trajectory generation for unmanned air vehicles," in *IEEE Conference on Decision and Control*, IEEE, 2003.

[2] A. Eele and A. Richards, "Path-planning with avoidance using non-linear branch-and-bound optimization," *Journal of Guidance, Control, and Dynamics*, vol. 32, pp. 384–394, Mar. 2009.

[3] A. Bicchi and L. Pallottino, "On optimal and cooperative conflict and resolution for and air traffic and management systems," *IEEE Transactions on Intelligent Transportation Systems*, vol. 1, no. 4, pp. 221–232, 2000.

[4] A. Raghunathan, V. Gopal, D. Subramanian, L. Biegler, and T. Samad, "Dynamic optimization strategies for three-dimensional conflict resolution of multiple aircraft," *Journal of Guidance, Control, and Dynamics*, vol. 27, no. 4, pp. 586–594, 2004.

[5] L. Biegler, "An overview of simultaneous strategies for dynamic optimization," *Chemical Engineering and Processing*, vol. 46, pp. 1043–1053, 2007.

[6] Y. Kuwata and J. How, "Three dimensional receding horizon control for UAVs," in *AIAA Guidance, Navigation, and Control Conference and Exhibit*, 2004.

[7] F. Borrelli, D. Subramanian, A. U. Raghunathan, and L. T. Biegler, "MILP and NLP techniques for centralized trajectory planning of multiple unmanned air vehicles," in *Proceedings of the 2006 American Control Conference*, IEEE, 2006.

[8] R. B. Patel and P. J. Goulart, "Trajectory generation for aircraft avoidance maneuvers using online optimization," *Journal of Guidance, Control, and Dynamics*, vol. 34, pp. 218–230, JanuaryFebruary 2011.

[9] A. Richards and J. How, "Aircraft trajectory planning with collision avoidance using mixed integer linear programming," in *American Control Conference, 2002. Proceedings of the*, pp. 1936–1941, 2002.

[10] A. Richards and J. How, "Decentralized model predictive control of cooperating UAVs," in *43rd IEEE Conference on Decision and Control*, IEEE, 2004.

[11] B. Fornberg, *A practical guide to pseudospectral methods,*, vol. 1 of *Cambridge Monographs on Applied and Computational Mathematics*. Cambridge University Press, 1996.

[12] Q. Gong, F. Fahroo, and M. Ross, "Spectral algorithm and for pseudospectral and methods and in optimal and control," in *Journal of Guidance, Control, and Dynamics*, vol. 31, May–June 2008.

[13] F. Fahroo and M. I. Ross, "Direct trajectory optimization by a chebyshev pseudospectral method," in *Proceedings of the American Control Conference*, 2000.

[14] J.-P. Berrut and L. Trefethen, "Barycentric lagrange and interpolation," *SIAM Review*, vol. 46, no. 3, pp. 501–517, 2004.

[15] G. T. Huntington and D. Benson, "A comparison of accuracy and computational efficiency of three pseudospectral methods," in *Proceedings of the AIAA Guidance, Navigation and Control Conference and Exhibit*, 2007.

[16] A. Wächter and L. Biegler, "Global and local convergence of line search filter methods for nonlinear programming," Tech. Rep. B-01-09, Carnegie Mellon University, 2002.

[17] O. Khatib, "Real-time obstacle avoidance for manipulators and mobile robots," *The International Journal of Robotics Research*, vol. 5, no. 1, pp. 90–98, 1986.

[18] A. Rahmani, K. Kosuge, T. Tsukamaki, and M. Mesbahi, "Multiple UAV deconfliction via navigation functions," in *AIAA Guidance, Navigation and Control Conference and Exhibit*, 2008.

[19] Y. Koren and J. Borenstein, "Potential field methods and their inherent limitations for mobile robot navigation," in *Robotics and Automation, 1991. Proceedings., 1991 IEEE International Conference on*, pp. 1398–1404 vol.2, 1991.

[20] M. H. Maia and R. K. H. Galvao, "On the use of mixed-integer linear programming for predictive control with avoidance constraints," *International Journal of Robust and Nonlinear Control*, vol. 19, no. 7, pp. 822–828, 2009.